Device Asymmetries and the Effect of the Rotor Run-up in a Two-plane Automatic Ball Balancing System

D.J. Rodrigues[a,*], A.R. Champneys[a], M.I. Friswell[b] and R.E. Wilson[a]

[a]Department of Engineering Mathematics, [b]Department of Aerospace Engineering,
University of Bristol, Bristol, BS8 1TR, UK

Abstract

We present a numerical investigation of a two-plane automatic ball balancer (ABB) for rotating machinery. This device consists of a pair of circular races that are set perpendicular to the shaft in two distinct planes. Within each race are a series of balancing balls which move to compensate any mass imbalance arising from rotor eccentricity or misalignment. We build upon an earlier bifurcation analysis of the steady state dynamics to consider device asymmetries such as non equal ball masses and we also investigate the effect of the rotor run-up.

1 Introduction

An automatic ball balancer (ABB) is a device which reduces vibrations in rotating machinery by compensating for the mass imbalance of the rotor. The ABB consists of a series of balls that are free to travel around a race which is set at a fixed distance from the shaft. During balanced operation the balls find such positions that the principal axis of inertia is repositioned onto the rotational axis. Because the imbalance does not need to be determined beforehand ABB's are ideally suited to applications where the amount of imbalance varies with the operating conditions. For example, automatic balancers are currently used in optical disk drives, machine tools and washing machines.

The first study of an ABB was carried out by Thearle in 1932 [1], and Lee and Van Moorhem demonstrated the existence of a stable balanced steady state at rotation speeds above the first critical frequency in a theoretical and experimental analysis [2]. However, in some cases the ABB may not balance the system even when operating at supercritical rotation speeds [3]. In 1977, Hedaya and Sharp [4] extended the autobalancing concept by proposing a two-plane device that can compensate for both shaft eccentricity and shaft misalignment, see Fig 1. Misalignment induces tilting vibrations and so models based on a 4DOF rotor which include gyroscopic effects must be considered [5, 6, 7]. In a previous study we use Lagrange's method and rotating coordinates to derive an autonomous set of governing equations [8]. A symmetric system is then considered and numerical continuation techniques are used to map out the stability boundaries of the balanced state in various parameter planes. The setup on a real machine is, however, usually asymmetric, for example the balls may have different masses or the balancing planes may not be equally spaced. Here we shall extend our work by considering the effect of these asymmetries and in addition we shall investigate the influence of the rotor run-up [9].

The rest of this paper is organised as follows. In section 2 we present and discuss the equations of motion for the ABB. The steady states of the system are considered in section 3, and we focus on using numerical bifurcation theory to investigate the effect that the physical parameters have on their stability. The effects of the rotor run-up are then investigated in section 4 and finally we draw conclusions and discuss possible directions for future work in section 5.

*Corresponding author. E-mail: david.rodrigues@bristol.ac.uk

2 Equations of motion

The setup of the ABB is illustrated in Fig. 1, and is based on a rigid rotor which has been fitted with a two-plane automatic balancer. The rotor has mass M, moment of inertia tensor $diag[J_t, J_t, J_p]$, and is mounted on two compliant linear bearings which are located at S_1 and S_2. The automatic balancer consists of a pair of races that are set normal to the shaft in two separate planes. Each race contains two balancing balls of mass m_i, which move through a viscous fluid and are free to travel, at a fixed distance R_i from the shaft axis. The position of the ith ball is specified by the axial and angular displacements z_i and α_i, which are written with respect to the $C\xi\eta z$ rotor axes.

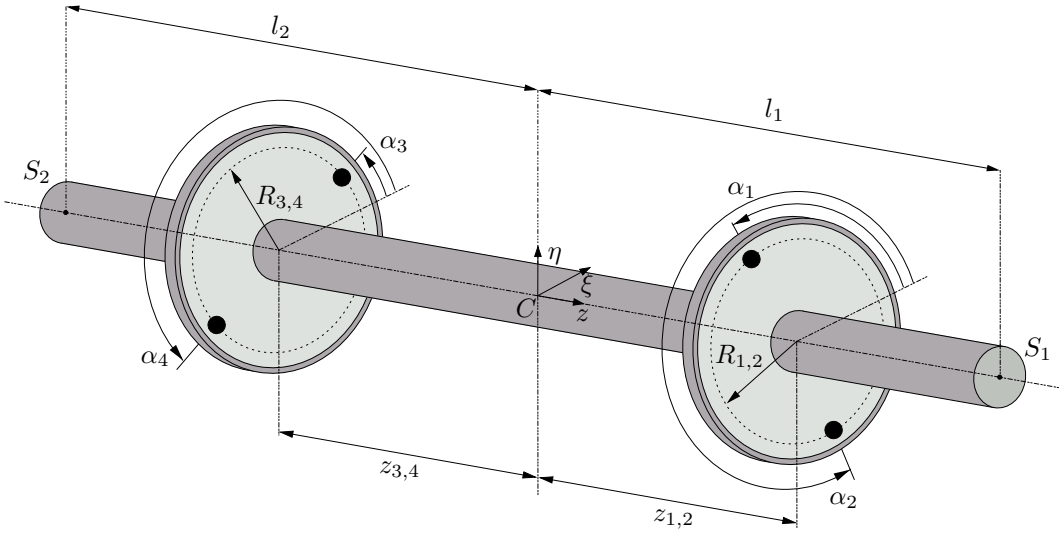

Fig. 1: Schematic diagram of a two-plane automatic balancer.

The equations of motion have been derived in [7, 8] using Lagrange's method and they can be written in the inertial space frame as

$$\mathbf{M}\ddot{\mathbf{q}} + (\mathbf{C} - i\dot{\varphi}_0\mathbf{G})\,\dot{\mathbf{q}} + \mathbf{K}\mathbf{q} = (\dot{\varphi}_0^2 - i\ddot{\varphi}_0)\mathbf{f}_I e^{i\varphi_0} + \sum_{k=1}^{4}(\dot{\varphi}_k^2 - i\ddot{\varphi}_k)\mathbf{f}_{b_k} e^{i\varphi_k}, \tag{1}$$

$$\tilde{J}_p\ddot{\varphi}_0 + c_r\dot{\varphi}_0 + \sum_{k=1}^{4} c_b(\dot{\varphi}_0 - \dot{\varphi}_k) + \Im((\ddot{\mathbf{q}}\cdot\mathbf{f}_I)e^{-i\varphi_0}) = L(\dot{\varphi}_0), \tag{2}$$

$$m_k R_k^2\ddot{\varphi}_k + c_b(\dot{\varphi}_k - \dot{\varphi}_0) + \Im\left((\ddot{\mathbf{q}}\cdot\mathbf{f}_{b_k})\,e^{-i\varphi_k}\right) = 0, \quad k = 1,\ldots,4. \tag{3}$$

Here $\mathbf{q} = [X + iY, \phi_Y - i\phi_X]^{\mathrm{T}}$ is the (complex) vector of the vibrational degrees of freedom[1], φ_0 is the rotor angle and $\varphi_k = \varphi_0 + \alpha_k$ is the angular displacement of the kth ball. The mass, gyroscopic, damping and stiffness matrices are given respectively by

$$\mathbf{M} = \begin{bmatrix} M & 0 \\ 0 & J_t \end{bmatrix} + \sum_{k=1}^{4}\begin{bmatrix} m_k & m_k z_k \\ m_k z_k & m_k z_k^2 \end{bmatrix}, \quad \mathbf{G} = \begin{bmatrix} 0 & 0 \\ 0 & J_p \end{bmatrix}, \quad \mathbf{C} = \begin{bmatrix} c_{11} & c_{12} \\ c_{12} & c_{22} \end{bmatrix}, \quad \mathbf{K} = \begin{bmatrix} k_{11} & k_{12} \\ k_{12} & k_{22} \end{bmatrix},$$

and the mass imbalance and ball vectors are given by

$$\mathbf{f}_I = \begin{bmatrix} M\epsilon e^{i\beta_1} \\ \chi\,(J_t - J_p)\,e^{i\beta_2} \end{bmatrix} \quad \text{and} \quad \mathbf{f}_{b_k} = \begin{bmatrix} m_k R_k \\ m_k R_k z_k \end{bmatrix}, \quad k = 1,\ldots 4.$$

Here ϵ and χ are the rotor eccentricity and misalignment respectively and $\beta_{1,2}$ are the fixed phases of these imbalances with respect to the rotor ξ axis. In addition, $\tilde{J}_p = J_p + J_t\chi^2 + M\epsilon^2$ is the modified polar

[1] As defined in [10]

moment of inertia, $L(\dot{\varphi}_0)$ is the driving torque generated by the motor and c_r is the torque damping. Finally c_b is the viscous damping of the balls in the race as they move through the fluid. We note that by taking $m_k = 0$ in (1), we recover the equations of motion for a four degree of freedom rotor [10]. Also, by setting the tilt angles $\phi_x = \phi_y \equiv 0$, the system reduces to the equations of motion for the planar automatic balancer [11]. The form of the governing equations suggest that automatic balancing can be viewed as a synchronization phenomena of coupled rotors [12]. For smooth operation we require that the ball speeds $\dot{\varphi}_k$ synchronize with the rotor speed $\dot{\varphi}_0$ and furthermore that the phases of the balls $\varphi_k - \varphi_0$ are such that their forcing cancels out, or at least reduces, the forcing from the rotor imbalance.
It is usual to assume that the motor can provide enough torque to realise a given angular velocity profile and so we shall impose the spin speed $\Omega(t) = \dot{\varphi}_0(t)$ instead of considering (2) with a given driving torque. Also in order to aid the stability analysis we can use the transformation $\mathbf{r} = \mathbf{q}e^{-i\varphi_0}$ to rewrite the equations of motion in the rotating frame to give

$$\begin{aligned}
&\mathbf{M}\ddot{\mathbf{r}} + \left[\mathbf{C} + i\Omega\left(2\mathbf{M} - \mathbf{G}\right)\right]\dot{\mathbf{r}} + \left[\mathbf{K} - \Omega^2\left(\mathbf{M} - \mathbf{G}\right) + i\left(\dot{\Omega}\mathbf{M} + \Omega\mathbf{C}\right)\right]\mathbf{r} \\
&\qquad = (\Omega^2 - i\dot{\Omega})\mathbf{f}_I + \sum_{k=1}^{4}\left[(\Omega + \dot{\alpha}_k)^2 - i\left(\dot{\Omega} + \ddot{\alpha}_k\right)\mathbf{f}_I e^{i\alpha_k}\right], \qquad (4) \\
&m_k R_k^2(\dot{\Omega} + \ddot{\alpha}_k) + c_b\dot{\alpha}_k + \Im\left\{\left[\left(\ddot{\mathbf{r}} + 2i\Omega\dot{\mathbf{r}} - \left(\Omega^2 - i\dot{\Omega}\right)\mathbf{r}\right)\cdot\mathbf{f}_{b_k}\right]e^{-i\alpha_k}\right\} = 0, \quad k = 1, \ldots, 4.
\end{aligned}$$

In the remainder of this paper we shall investigate the model given by equation (4), however we note that many effects such as bearing anisotropy, geometric defects and dry friction between the race and balls are not included. We refer the interested reader to [13, 14, 15].

3 Bifurcation analysis of the balanced steady state

Steady state solutions are obtained by setting all time derivatives in the equations of motion (4) to zero. Moreover, if we also set the vibrational coordinates $\mathbf{r} = \mathbf{0}$, we arrive at the following condition for a balanced steady state

$$\mathbf{f}_I + \sum_{k=1}^{4}\mathbf{f}_{b_k}e^{i\alpha_k} = 0. \qquad (5)$$

Of course this equation simply states that the forces and moments acting on the rotor due to the imbalance and balancing balls must be in equilibrium. The solution is physically unique and exists provided that the balls have a mass large enough to cope with the imbalance. The ball positions $\boldsymbol{\alpha} = \boldsymbol{\alpha}^*$ can be determined in closed form but the equations are long and so are not presented here. Next we shall use the continuation package `AUTO` [16] to compute bifurcation diagrams showing the regions of stability in various parameter planes. The boundaries of stability are formed by Hopf bifurcations which mark the onset of rotor vibrations.
Unless otherwise stated, for the rest of this study we shall consider an ABB model with the following parameters

$$\begin{aligned}
&M = 1, \quad R_k = R = 1, \quad k_{11} = 1, \quad l_1 = l_2 = 3, \quad z_{1,2} = z_{3,4} = 2, \\
&m_k = m, \quad \mathbf{K} = \begin{bmatrix} 1 & 0 \\ 0 & 9 \end{bmatrix}, \quad c = 0.02 \quad \text{where} \quad \mathbf{C} = c\mathbf{K} \quad \text{and} \quad \bar{c}_b \equiv \frac{c_b}{m} = 0.01.
\end{aligned} \qquad (6)$$

The first three constraints are simply rescalings which make the equations identical to the nondimensionalised version. The stiffness and damping values are based on a rotor with two equal isotropic bearings where the center of mass is located at the midspan and the shaft has a length of six times the race radius. The approximate critical frequencies for the cylindrical and conical whirls occur respectively at

$$\Omega_1 = \sqrt{\frac{k_{11}}{M}} \equiv 1, \quad \text{and} \quad \Omega_2 = \sqrt{\frac{k_{22}}{J_t - J_p}}. \qquad (7)$$

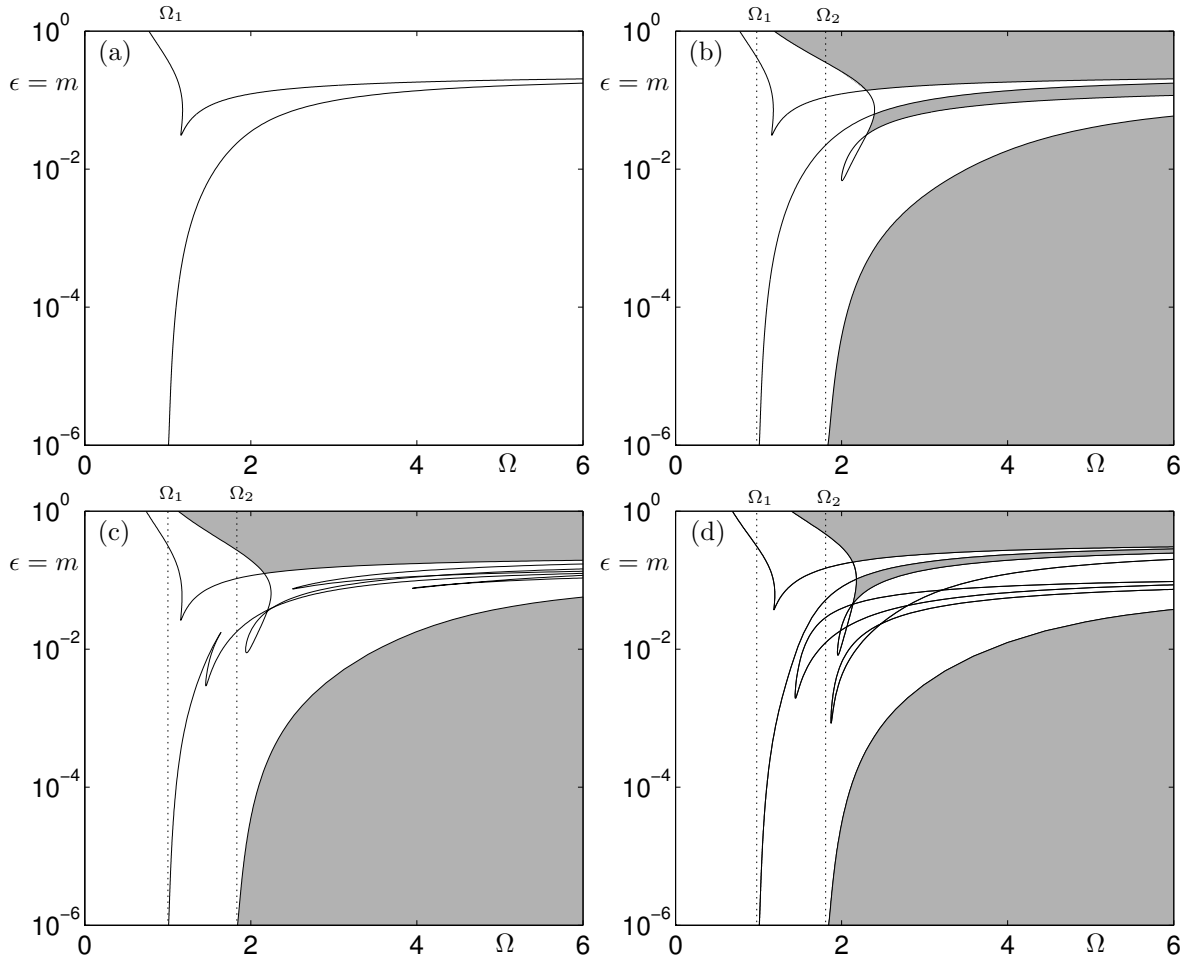

Fig. 2: Bifurcation diagrams showing stable regions of the balanced state (shaded) in the case of a static imbalance. The eccentricity ϵ is varied against Ω, whilst m is kept equal to ϵ so that $\boldsymbol{\alpha}^*$ remains constant. Panel (a) is a bifurcation diagram for a 'disk' type rotor $J_p > J_t$ and panel (b) is for a 'long' type rotor $J_p < J_t$. Similar diagrams for the 'long' type rotor are shown in (c) where one of the balls has a mass 20% greater than the others and in (d) where $z_{1,2} = 1$ and $z_{3,4} = 3$ so that the balancing planes are not equidistant from the midspan.

Figure 2 shows stability diagrams for the static imbalance case (i.e. an imbalance with no misalignment $\chi = 0$). The eccentricity ϵ, is plotted against Ω, whilst we also vary the ball mass so that $m = \epsilon$. Thus, the mass of the balls scales with the imbalance and the balanced state $\boldsymbol{\alpha}^*$ does not change value. A logarithmic scale is used for the vertical axis so that a wide range of eccentricities can be considered. Panel (a) shows the situation for a 'disk' type rotor where $J_p > J_t$, here there is no stable region of balanced operation because the influence of the gyroscopic term is such that the eigenfrequency corresponding to the conical whirl is always greater than the rotor speed Ω. This means that there is no conical critical speed Ω_2 and thus no associated self-aligning process[2], hence the ABB is not stabilised with respect to conical motions. The method of direct separation of motion has been used by Sperling *et al.* [12] to derive this result and in addition they discuss how it relates to Blekhman's generalised self-balancing principle [17]. From a practical viewpoint however, the prognosis for the autobalancing of 'disk' type rotors is not as bad as it may first seem. Because the conical mode has no associated critical speed, 'disk' rotors often need only to be balanced with respect to the static unbalance and a single plane ABB can be used to provide a partial unbalance compensation [18].

[2]Self aligning is the phenomena whereby a rotor will tend to rotate about its principal axis of inertia at supercritical rotation speeds.

Next we illustrate in panel (b) the case for a 'long' rotor where $J_p < J_t$. We have taken $J_t = 3.25$ and $J_p = 0.5$ which corresponds to a solid cylindrical rotor with a height of six times its radius. For these values the critical speed corresponding to the conical whirl occurs at $\Omega_2 \simeq 1.81$. Here there are several regions of balanced operation though for applications the main area of interest occurs where there is a large connected stable region for small eccentricities and supercritical rotation speeds. The Hopf curve which bounds this region asymptotes towards $\Omega = \Omega_2$ as $\epsilon \to 0$, hence there is no stable region in the subcritical regime. We note at this point that these results for the stability of the balanced state are only valid *locally* and there most likely exists competing dynamics in much of the stable range. We shall now investigate how asymmetries of the ABB device can effect its stability. Panel (c) shows the situation where one of the balls has a mass 20% greater than the other balls. We see that the stable regions remain largely unchanged, however extra Hopf instability curves are present. These arise because the introduction of a different ball mass breaks the symmetry of the system. Another factor which must be noted is that unequal balls cannot counterbalance each other by settling to opposite sides of the race. Thus the overall capability of the ABB is reduced as unequal balls will inevitably add an imbalance to a rotor that is already well balanced [19]. Next the diagram in panel (d) shows the case where the balancing planes are not equally spaced from the midspan. We have taken $z_{1,2} = 1$ and $z_{3,4} = 3$, and again the main point to note is the robustness of the stable region for low eccentricities and supercritical rotation speeds. We shall now return to the symmetric ABB setup but consider a rotor that suffers from

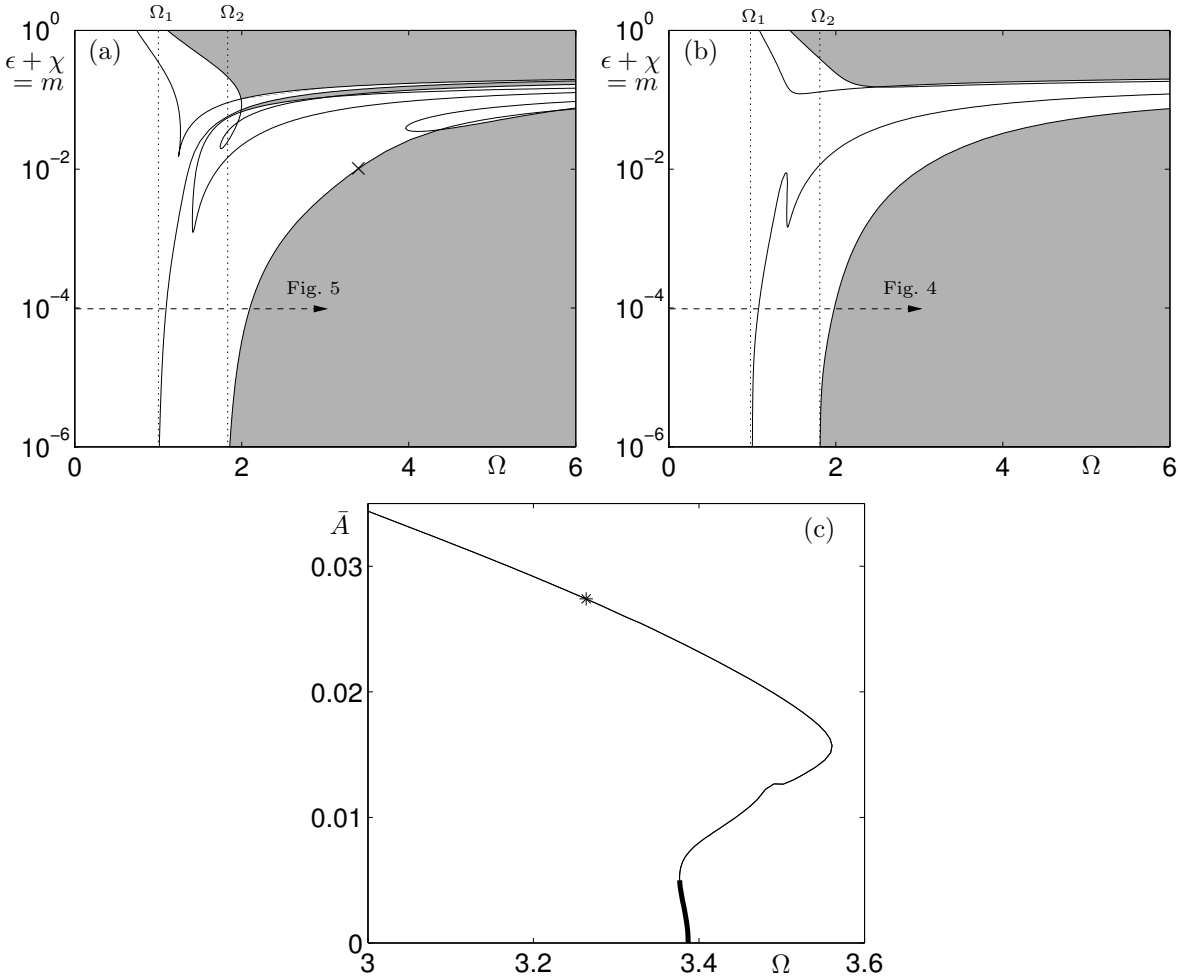

Fig. 3: Bifurcation diagrams in the case of a 'long' rotor with a dynamic imbalance. Panel (a) is for a race damping value of $c_b = 0.01$ and panel (b) is for a higher race damping value of $c_b = 0.1$. The limit cycle which emanates from the Hopf bifurcation marked by a $\times$ is continued in panel (c) and the indicated one-parameter sweeps in Ω are illustrated in Figs. 4 and 5.

a dynamic imbalance (i.e. an imbalance with both an eccentricity ϵ and a misalignment χ). Similar plots to those of Fig. 2 are illustrated in Fig. 3 for the dynamic imbalance case with $m = \epsilon + \chi$, $\epsilon = \chi$ and a constant phase $\beta_1 = 1$. In panel (a) the race damping parameter is $c_b = 0.01$ whereas for panel (b) the race damping value is increased to $c_b = 0.1$. As a result much of the complicated structure in the high eccentricity regime is smoothed out although the main influence of this parameter is manifest in the transient dynamics and in the size of the basin of attraction of the balanced state. The limit cycle which is born at the marked Hopf bifurcation for $c_b = 0.01$ and $m = 0.01$ is continued in panel (c), here $\bar{A}$ is the average rotor vibration at points one unit length from the midspan. The Hopf bifurcation is supercritical and so there is a (small) region where the limit cycle is stable. In a controlled experiment we would expect to see small oscillations of the balls about their balanced positions before the balls would desynchronize with the rotor. For smaller values of the imbalance, say $\epsilon + \chi = 1 \times 10^{-4}$, the Hopf bifurcation is subcritical and the transition to the desynchronized state would be immediate. The ability to follow the desynchronized limit cycles with continuation software is a work in progress.

4 The effect of the rotor run-up

In this section we consider the effect of the rotor run-up on the vibrations of the system. In Fig. 4 we plot the absolute ball speeds $\dot{\varphi}_k$ against the rotor speed Ω for the sweep shown in Fig. 3 (b) with the race damping value of $c_b = 0.1$. The mass of the balls is $m = 1 \times 10^{-4}$ and we *slowly* increase the rotor speed over a time scale of $t = 1 \times 10^4$ corresponding to approximately 3 hours. Here we can see that the

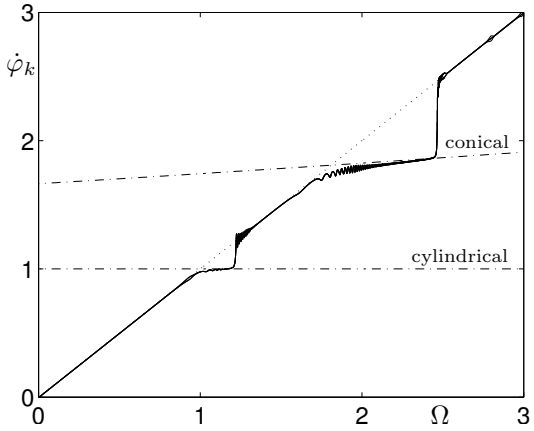

Fig. 4: Diagram showing the ball speeds $\dot{\varphi}_k$ against rotor speed Ω for the dynamic imbalance case with $c_b = 0.1$ and $m = 1 \times 10^{-4}$.

ball speeds initially synchronize with the rotor, however as the rotor approaches and passes through its critical speeds the balls tend to 'stall' and synchronize with the rotor eigenfrequencies. As the rotation speed is increased still further the balls again resynchronize with the rotor. If the race damping value is too low, say $c_b = 0.01$, then the balls may never resynchronize with the rotor and they stay at the eigenfrequency speed. This behaviour was first analysed in [20] and is similar to the Sommerfeld effect in which a rotating machine with an insufficiently powerful motor has difficulty in passing through the critical speeds.
The optimization of the velocity profile for a particular application lies outside the scope of this paper, however we shall now consider a more realistic rotor run-up that we can model by the Hill function

$$\Omega(t) = \Omega_{max} \frac{t^n}{t_{1/2}^n + t^n}. \tag{8}$$

This function is plotted in Fig. 5 (a) for the parameter values $(\Omega_{max}, t_{1/2}, n) = (3, 10, 3)$, note that $\Omega \approx 0.9\Omega_{max}$ for $t = 20$. We use this rotor run-up to perform the indicated sweep through Fig. 3 (a) for the race damping value of $c_b = 0.01$. The results are shown in Fig. 5 (b) and (c), initially the

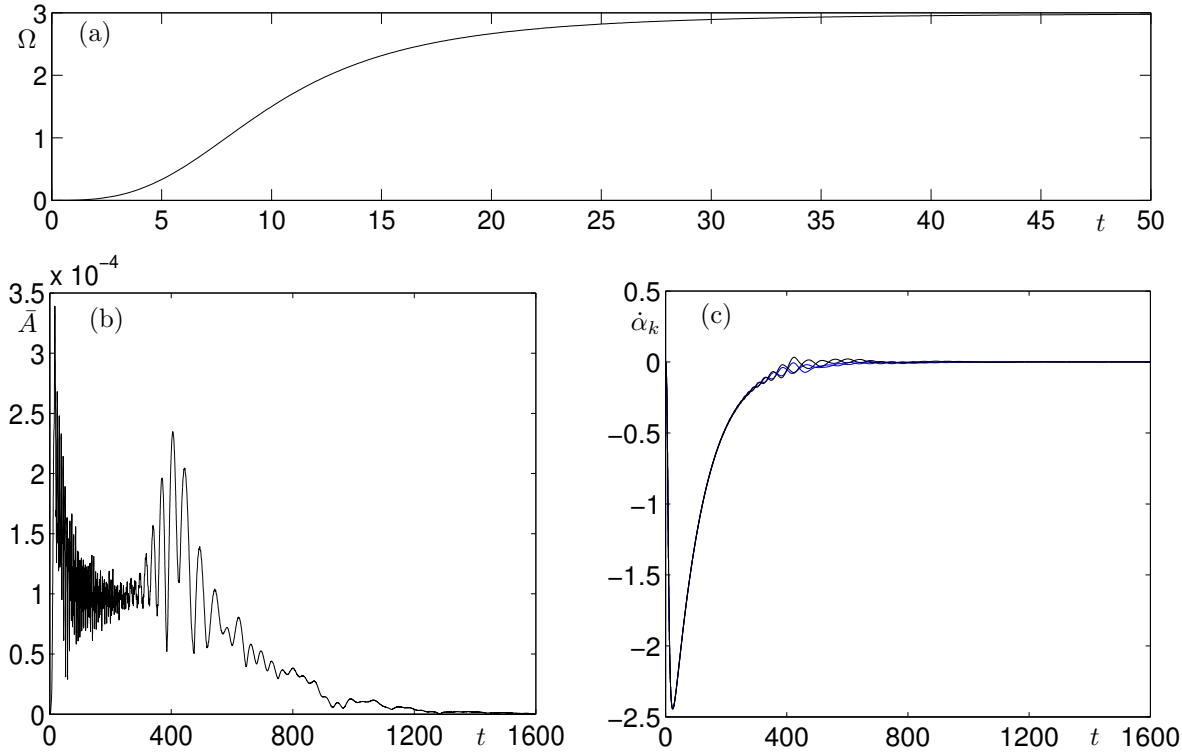

Fig. 5: Simulations which in include the effect of rotor run-up. Panel (a) shows the considered angular velocity profile and panels (b) and (c) display respectively the amplitude of rotor vibrations $\bar{A}$ and the relative ball speeds $\dot{\alpha}_k = \dot{\varphi}_k - \dot{\varphi}_0$.

balls speeds lag behind behind the rotor but eventually the balls catch up synchronizing with the rotor, furthermore they have phases which compensate for the rotor imbalance. It is interesting that there is a period of increased vibrations as the balls approach the rotor speed $\dot{\varphi}_0$. This occurs because the balls desynchronize with each other before resynchronizing with the rotor. However, the resulting vibrations can be significantly reduced if the race damping parameter is increased to say $c_b = 0.1$. Ideally a value of c_b should be chosen so that the balls are close to being critically damped [21], however realising this aim in practice may prove difficult. If the balls undergo non-synchronous motions and complete many circuits of the race then energy will be dissipated in the fluid causing it to heat up and its viscosity to decrease.

5 Conclusion

We have used rotating complex coordinates to present a simple model for a rigid rotor with a two-plane ABB. Stability charts obtained by numerical continuation of the Hopf bifurcation curves together with simulations show that the considered device can effectively eliminate imbalances arising from both shaft eccentricity and shaft misalignment. Furthermore, the introduction of ball mass asymmetry or balancing planes that are not equally spaced has little effect on the stable region provided that the machine is operating in the supercritical regime with typical values for the eccentricities[3]. Our investigations of the rotor run-up highlights the phenomena of non-synchronous motions near critical speeds and also the presence of increased vibrations as the balls desynchronize with each other in order to resynchronize with the rotor speed. To eliminate the non-synchronous motions completely one could envisage using a partitioned race [22] or a clamping mechanism where the balls would be fixed until supercritical rotation speeds are reached [1].

[3]For machine tools and aircraft gas turbines $\epsilon \simeq 1 \times 10^{-5}$

We plan to continue the present work by investigating the symmetry properties of the bifurcations which give rise to the balanced state. Normal form theory and the equivariant branching lemma can then be used to give explicit conditions for the stability of the bifurcating solutions. The global stability properties of the system will also be investigated through the use of Lyapunov functions and experimental work is currently in progress in order that we may verify our findings and determine the influence of other effects such as ball-race interactions and rotor flexibility.

6 Acknowledgements

The authors are grateful to Rolls-Royce plc. for financial support of this research.

References

[1] E. Thearle, A new type of dynamic-balancing machine, *Transactions of the ASME* **54**(APM-54-12) (1932) 131-141.

[2] J. Lee and W. K. Van Moorhem, Analytical and experimental analysis of a self compensating dynamic balancer in a rotating mechanism, *ASME Journal of Dynamic Systems, Measurement and Control* **118** (1996) 468-475.

[3] J. Chung and D. S. Ro, Dynamic analysis of an automatic dynamic balancer for rotating mechanisms. *Journal of Sound and Vibration* **228**(5) (1999) 1035-1056.

[4] M. Hedaya and R. Sharp, An analysis of a new type of automatic balancer, *Journal of Mechanical Engineering Science* **19**(5) (1977) 221-226.

[5] J. Chung and I. Jang, Dynamic response and stability analysis of an automatic ball balancer for a flexible rotor. *Journal of Sound and Vibration* **259**(1) (2003) 31-43.

[6] C.-P. Chao, Y.-D. Huang, and C.-K. Sung, Non-planar dynamic modeling for the optical disk drive spindles equipped with an automatic balancer. *Mechanism and Machine Theory* **38** (2003) 1289-1305.

[7] L. Sperling, B. Ryzhik, Ch. Linz and H. Duckstein, Simulation of two-plane automatic balancing of a rigid rotor, *Mathematics and Computers in Simulation* **58** (2002) 351-365.

[8] D. J. Rodrigues, A. R. Champneys, M. I. Friswell and R. E. Wilson, Automatic two-plane balancing for rigid rotors. *International Journal of Nonlinear Mechanics* (in press)

[9] J. Chung, Effect of gravity and angular velocity on an automatic ball balancer. *Proc. IMechE Part C: J. Mechanical Engineering Science* **219** (2005) 43-51.

[10] G. Genta, *Dynamics of Rotating Systems*. Springer, New York (2005).

[11] K. Green, A. R. Champneys, and N. J. Lieven, Bifurcation analysis of an automatic dynamic balancer for eccentric rotors. *Journal of Sound and Vibration* **291** (2006) 861-881.

[12] L. Sperling, F. Merten and H. Duckstein, Self-synchronization and automatic balancing in rotor dynamics, *International Journal of Rotating Machinery* **6**(4) (2000) 275-285.

[13] B. Ryzhik, L. Sperling, and H. Duckstein, Auto-balancing of anisotropically supported rigid rotors, *Technische Mechanik* **24** (2004) 37-50.

[14] K-O. Olsson, Limits for the use of auto-balancing, *International Journal of Rotating Machinery* **10**(3) (2004) 221-226.

[15] N. Van De Wouw, M. N. Van Den Heuvel, H. Nijmeijer and J. A. Van Rooij, Performance of an automatic ball balancer with dry friction, *International Journal of Bifurcation and Chaos* **20**(1) (2005) 65-85.

[16] E. Doedel, A. Champneys, T. Fairgrieve, Y. Kusnetsov, B. Sanstede,
and X. Wang, AUTO97: Continuation and bifurcation software for ordinary differential equations, `http://indy.cs.concordia.ca/auto/main.html`, 1997.

[17] I. Blekhman, *Vibrational Mechanics*. World Scientific (2000).

[18] L. Sperling, B. Ryzhik and H. Duckstein, Single-plane auto-balancing of rigid rotors, *Technische Mechanik* **24** (2004) 1-24.

[19] R. Horvath, G. T. Flowers and J. Fausz, Influence of nonidealities on the performance of a self-balancing rotor system. *Proc. of IMECE* (2005).

[20] B. Ryzhik, L. Sperling, and H. Duckstein, Non-synchronous motions near critical speeds in a single-plane auto-balancing device. *Technische Mechanik* **24** (2004) 25-36.

[21] D. J. Rodrigues, A. R. Champneys, M. I. Friswell and R. E. Wilson, Automatic balancing of a rigid rotor with misaligned shaft *Applied Mechanics and Materials* **5-6** (2006) 231-236.

[22] K. Green, A. R. Champneys, and M. I. Friswell, Analysis of the transient response of an automatic ball balancer for eccentric rotors. *International Journal of Mechanical Sciences* **48** (2006) 274-293.